PUBLICATIONS OF THE ASTRONOMICAL SOCIETY OF THE PACIFIC, 111:321–334, 1999 March

The Orbit of 16 Cygni AB

HEATHER M. HAUSER[1,2] AND GEOFFREY W. MARCY[1,3]

Department of Physics and Astronomy, San Francisco State University, San Francisco, CA 94132

Received 1998 August 11; accepted 1998 November 24

ABSTRACT. The high orbital eccentricity of the planet around 16 Cygni B may have been induced by the companion star, 16 Cygni A, but only if the stellar binary has sufficiently small periastron distance. The long period of the stellar binary, $\sim 3 \times 10^4$ yr, implies that less than 1% of the orbit has transpired since its first astrometric measurements in 1830. Therefore, we compute the orbit from the measured instantaneous velocity and position vectors, based on new precise Doppler and astrometric data, along with the *Hipparcos* parallax. The only unknown parameter is the separation between AB along the line of sight, constrained by the demand that the orbit be bound, which leads to a family of possible orbits for 16 Cygni AB. The physically plausible orbits have 18,200 yr $< P <$ 1.3 Myr, 877 $< a <$ 15,180 AU, and periastron distances $68 < r_p < 1500$ AU. The orbit is definitely eccentric, with $e = 0.54$–0.96. All orbital parameters here are in approximate agreement with the previous computation by Romanenko. The new stellar binary orbit remains consistent with the possibility that perturbations from 16 Cygni A cause the eccentricity in the planet around 16 Cygni B. Recently a red point source has been detected 3.″2 from 16 Cygni A, but its membership remains unknown (Trilling et al.). We assess its membership based on astrometry and velocities of 16 Cygni A. The point source is either a low-mass M dwarf separated by ~ 80 AU from component A or it is a higher mass star of perhaps $\sim 0.5\ M_\odot$, separated by at least 150 AU from 16 Cygni A—indeed possibly a background star. If the new companion is bound, 16 Cygni A and B never approach each other closer than ~ 500 AU, which diminishes the prospects that 16 Cygni A induces the eccentricity of the planet around 16 Cygni B.

1. INTRODUCTION

The wide binary, 16 Cygni A and B (=HD 186408 and 186427, HIP 96895 and 96901, ADS 12815AB) consists of two G-type main-sequence stars separated on the sky by 39″, which implies an orbital period of at least 10^4 yr (Romanenko 1994; Kiselev & Romanenko 1996). The detection of a planetary companion around component B (Cochran et al. 1997; Marcy & Butler 1998) has cast considerable interest on this stellar binary system as a testing ground for theories of planet formation and orbital evolution. The large eccentricity of the planetary orbit ($e = 0.69$) may be explained by gravitational perturbations imposed by stellar component A (Holman, Touma, & Tremaine 1997; Mazeh, Krymolowsky, & Rosenfeld 1997). Thus, the stellar binary orbit constitutes an important ingredient in understanding the formation and orbit of the planet.

There is an obvious difficulty in determining orbital parameters for periods greater than 10,000 yr. Only a small fraction of the orbit has transpired since astrometric measurements were first obtained in the early 1800s. Given errors in measurements, the orbit is poorly constrained by astrometric observations that reveal only a small arc. Nonetheless, orbital determination is possible in principle, since Newtonian mechanics is deterministic given the position and velocity vectors for two specified point masses at just one instant of time. Observations obtained during a small portion of a full orbital period are sufficient to constrain the family of orbital parameters.

The extraordinary eccentricity ($e = 0.69$) of the planet around 16 Cygni B requires explanation, as conventional models of the formation of gas giants in a protostellar disk often predict dynamical circularization of the orbit (Cochran et al. 1997; Artymowicz 1998). If the planet, 16 Cygni Bb, indeed formed in a nearly circular orbit with its orbital plane inclined to the plane of the stellar binary by at least 45°, then the planetary orbit oscillates between high- and low-eccentricity states (Holman et al. 1997; Mazeh et al. 1997). This effect occurs only if there are no other planets with $M \approx M_{\rm Jup}$ within 30 AU. The timescale for the orbital oscillations is expected to be 10^7–10^{10} yr, depending on the

[1] Visiting Astronomer, Lick Observatory, operated by the University of California.

[2] Currently at Department of Physics and Astronomy, University of Oregon, Eugene, OR 97403.

[3] Also at Department of Astronomy, University of California, Berkeley, Berkeley, CA 94720; gmarcy@etoile.berkeley.edu.

detailed orbit of the stellar binary. Holman et al. examined the variation of the inclination and eccentricity of the planetary orbit for two possible values of the binary periastron distance, 100 and 500 AU. Further investigation of this possible explanation for the highly eccentric planetary orbit depends on the true periastron distance and the period of the 16 Cygni AB binary orbit.

The orbit of 16 Cygni AB has been difficult to determine, as reliable astrometric data cover less than 1% of the orbit. An orbital solution was computed by Romanenko (1994) and by Kiselev & Romanenko (1996) who used 33 astrometric observations spanning the years 1832–1990 and employed a few radial velocity measurements with precision of ~ 300 m s^{-1}. They find an orbital period in the likely range $P = 30{,}000$–$132{,}000$ yr (though possibly infinite), a semimajor axis in the range $a = 1200$–3300 AU, and an eccentricity in the range $e = 0.70$–0.96. Somewhat suspiciously, they find that the time of periastron passage occurred within 1000 yr of the present, which is less than 3% of the orbital period. We can think of no selection effect that would tend to favor detection of binaries near their time of periastron passage, especially for equal-mass binaries that reside within 25 pc of the Sun.

A recent coronographic and infrared adaptive optics study of 16 Cygni A shows a nearby star located only 3.″2 away from it (Trilling, Brown, & Liu 1998). This new prospective component, "16 Cygni C" if bound to A, would be a low-mass star based on IR photometry, which suggests a mass $\sim 0.4 \pm 0.15\ M_{\odot}$ (Trilling et al. 1998). However, it may be a background star, presumably a K giant. As its membership remains unknown, we examine the available astrometry of 16 Cygni A for signs of perturbations caused by it.

It remains important to compute the orbit of AB alone, without the possible low-mass third star. The two-body orbit of A and B provides a well-defined dynamical model against which to compare the actual astrometry and velocities of the two stars. Any discrepancy or lack thereof would bear on the validity of the two-body model, thus providing dynamical information on any prospective third star in the system.

In this paper, we present new astrometric data and a precise relative radial velocity for the stellar components, A and B, along with the parallax and astrometry from *Hipparcos*. To determine the orbital parameters, we employ a revised orbital method, similar to that of Kiselev & Romanenko (1996) and Irwin, Yang, & Walker (1996). Section 2 contains a description of the extensive astrometric data, § 3 describes the new radial velocity measurements, § 4 contains a redetermination of the stellar masses, and § 5 describes our new orbital solution technique. In § 6 the family of orbits for 16 Cygni AB is determined. In § 7 we discuss the effects of any third star. In § 8 we discuss the status of the eccentricity of the planet around 16 Cygni B.

2. ASTROMETRIC DATA

C. E. Worley (1996, private communication of results from the Washington Double Star Catalog of Observations [WDSCO]) generously supplied 486 astrometric observations for 16 Cygni in machine-readable form from the Washington Double Star Catalog of Observations. From this catalog we have extracted the observation date, the position angle θ (deg) of B relative to A, the separation ρ (arcsec), the code for the observer or observatory, and the code for the observational method. We ignored one observation that was privately communicated to Worley. Figure 1 shows the variation of the position angle, θ, with time. The position angle is measured from north toward east to the position of the secondary. Figure 2 shows the raw measured values of ρ during the length of the data set. To account for

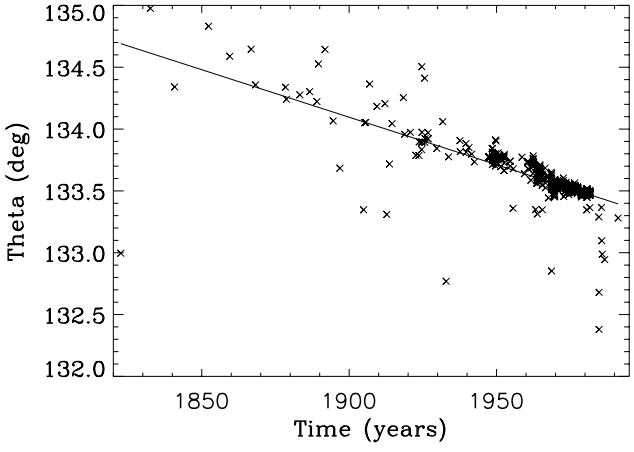

FIG. 1.—Position angle as measured from north toward east. First-order polynomial fit yields $\theta = \theta + \alpha(d\theta/dt)$, where $\theta = 164.6$(deg) and $\alpha = -0.00768$ deg yr^{-1}.

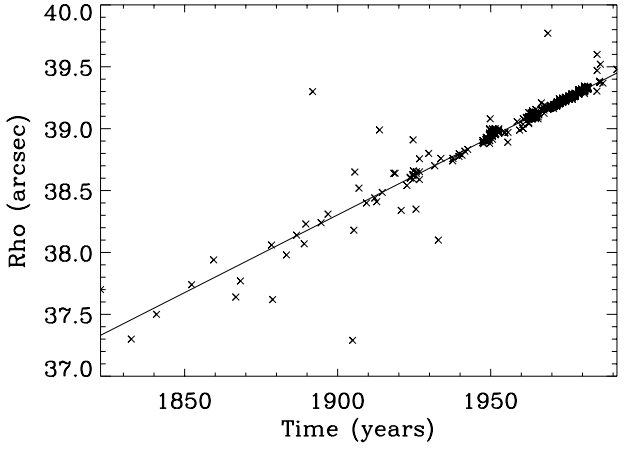

FIG. 2.—Angular separation of the 16 Cygni binary system. First-order polynomial fit yields $\rho = \rho + \beta(d\rho/dt)$, where $\rho = 14.35$(arcsec) and $\beta = 0.0126$ arcsec yr^{-1}.

precession of the coordinate system (Van den Bos 1962, Chap. 22), the values of θ are corrected to epoch 2000. These corrections are quite significant for θ, which changes by up to 1°.2 for the oldest values from 1832. We thank A. Irwin for comments about this correction.

To calculate the orbit of 16 Cygni B with respect to 16 Cygni A we determine θ and ρ, along with their uncertainties, at a specific time. We choose $t = 1981.77$ since there is a wealth of accurate data at that epoch. For both variables we used a linear least-squares and a Monte Carlo approach to estimate the instantaneous values and uncertainties, respectively. From this process we find values of $\theta = 133°.44 \pm 0°.014$ and $\rho = 39''.338 \pm 0''.0053$ for epoch 1981.77.

We now extract the velocity information from the astrometry. A linear fit to the astrometry provides $d\theta/dt$ and $d\rho/dt$ (slopes). The error analysis for $d\theta/dt$ and $d\rho/dt$ follows from Bevington & Robinson (1992). Since we cannot communicate with the original astronomers that did the 16 Cygni AB astrometry in the 1800s, we estimate the uncertainties in θ and ρ during the course of 164 yr to impose weights on the astrometric points. The weights are based on the measurement fluctuations during the first four epochs. Clearly a better method could be obtained by assigning weights that are associated with individual observers or observatories, but the resulting slopes would not change significantly. Table 1 shows the scatter and the resulting weights that were derived for the different portions of astrometric observations. From this method, we found that $d\theta/dt = -0°.00768 \pm 0°.00028$ yr^{-1} and $d\rho/dt = 12.6 \pm 0.16$ mas yr^{-1}.

Hipparcos astrometry (Perryman et al. 1997) provides an excellent check on the ground-based measurements. *Hipparcos* at epoch 1991.25 yields $\rho = 39''.451 \pm 0''.001$, $\theta = 133°.373 \pm 0°.002$, $d\rho/dt = 13.44 \pm 0.5$ mas yr^{-1}, and $d\theta/dt = -0°.008 \pm 0°.001$ yr^{-1}. These *Hipparcos* measurements agree with the extrapolation of ground-based values to epoch $t = 1991.25$, to within errors of a few mas. The *Hipparcos* measurements have roughly 10 times greater precision than ground-based work, but the longer time baseline of the latter renders the two sets comparable in value. Thus the *Hipparcos* measurements agree with, and do not alter or improve, the ground-based astrometry of 16 Cygni AB.

TABLE 1

WEIGHTS ADOPTED FOR $d\theta/dt$ AND $d\rho/dt$ CALCULATIONS

Epoch	σ_θ (deg)	w_i (θ) (deg^{-2})	σ_ρ (arcsec)	w_i (ρ) (arcsec^{-2})
1822–1947.....	0.5	4	0.5	4
1947–1962.....	0.05	400	0.05	400
1962–1982.....	0.05	400	0.02	2500
1982–1987.....	0.5	4	0.5	4
1987–1992.....	0.2	5	0.1	10

2.1. Converting Astrometry to Cartesian Coordinates

We transform from the polar coordinates of astrometry to Cartesian, physical dimensions using the measured parallax. The *Hipparcos* catalog (Perryman et al. 1997) gives a parallax for 16 Cygni A and B. We use a straight average of these two values and adopt a parallax for the 16 Cygni system of $\pi P = 46.475 \pm 0.50$ mas. The physical components of the Cartesian position vector are given by

$$x(\mathrm{AU}) = \frac{\rho}{\pi_P} \cos\theta \ ; \tag{1}$$

$$y(\mathrm{AU}) = \frac{\rho}{\pi_P} \sin\theta \ . \tag{2}$$

V_x and V_y are given by the time derivative of x and y, respectively. Using the small angle approximation, they are given by

$$V_x = \frac{1}{\pi_P}\frac{d\rho}{dt}\cos\theta - \frac{\rho}{\pi_P}\frac{d\theta}{dt}\sin\theta \ ; \tag{3}$$

$$V_y = \frac{1}{\pi_P}\frac{d\rho}{dt}\sin\theta + \frac{\rho}{\pi_P}\frac{d\theta}{dt}\cos\theta \ . \tag{4}$$

The observables $[\rho, \theta, d\rho/dt, d\theta/dt]$ are now in the desired form, $[x, y, V_x, V_y]$.

3. 16 CYGNI A AND B: RADIAL VELOCITY DIFFERENCE

During the past 10 yr at Lick Observatory we have monitored the Doppler shifts of 107 solar-type stars as part of a search for Jupiter-mass companions. We used the "Hamilton" coudé echelle spectrometer (Vogt 1987) and details of the Doppler measurements are described by Butler et al. (1996). To date, we have made 42 observations of 16 Cygni A and 80 observations of 16 Cygni B. Figures 3 and 4 show the Doppler data for the individual stars as a function of time during the past 11 yr. For 16 Cygni A (Fig. 3), there is no obvious velocity variation, except for a small downward trend of -4.1 ± 1.5 m s^{-1} yr^{-1}, which is significant at only the 2.7 σ level. Section 7 contains further discussion of this trend.

The velocities for 16 Cygni B (Fig. 4) exhibit Keplerian motion owing to the gravitational tug of a 1.76 $M_{\mathrm{Jup}}/\sin i$ planet in an $\sim$800 day eccentric orbit (Cochran et al. 1997). Figure 4 here shows the complete set of velocities from Lick Observatory. The residuals to the planetary orbit have an rms of 9.34 m s^{-1}, consistent with errors. A trend exists in the residuals during 11 yr of -1.2 m s^{-1} yr^{-1}, which is probably caused by systematic errors, as it appears in other program stars.

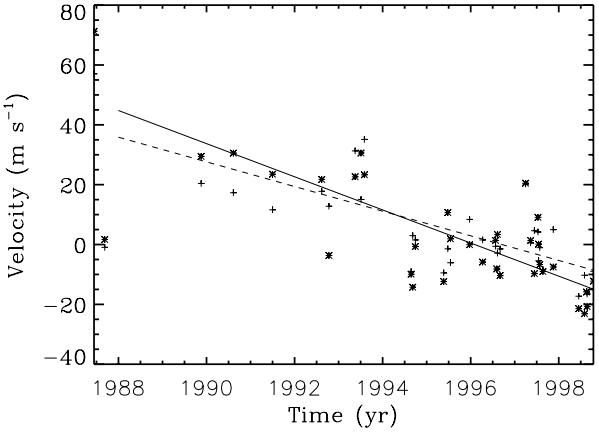

FIG. 3.—Relative velocities for 16 Cygni A (HR 7503 = HD 186408), showing 37 observations (from 1987 to the present). The asterisks show the raw velocities, and the associated linear fit (*solid line*) has a slope of -5.1 ± 1.5 m s^{-1} yr^{-1}. Systematic errors in the raw velocities were subtracted by using the residuals to the Keplerian fit to 16 Cygni B. The corrected velocities for 16 Cygni A are shown as plus signs, and the associated linear fit (*dashed line*) has a slope of -4.1 ± 1.5 m s^{-1} yr^{-1}. The rms to the linear fits to the raw and corrected velocities are 13.4 and 11.7 m s^{-1}, respectively.

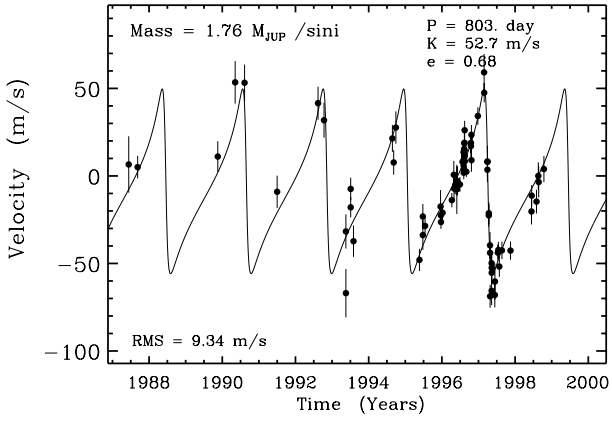

FIG. 4.—Doppler velocities for 16 Cygni B. The orbital fit for the planetary companion is shown with the solid line. The residuals to the orbital fit have an rms of 9.34 m s^{-1}, consistent with the errors.

The radial velocity difference between 16 Cygni B and A is computed in the following manner. Several hundred chunks of the 16 Cygni B spectrum, each 40 pixels long, are fitted with the corresponding chunks of the spectrum of 16 Cygni A. Both spectra were taken on 1995 July 1 (JD 2,449, 892.9). The free parameter in the fit to each chunk is the relative Doppler shift.

The final radial velocity of 16 Cygni B relative to A is the average of these shifts. This procedure returns the radial velocity difference (V_{B-A}) which is then corrected for the radial velocity component caused by the orbiting planet 16 Cygni Bb. We find $V_{B-A} = -524 \pm 10$ m s^{-1}, where negative value denotes that 16 Cygni B is moving toward us relative to A. Of the 700 spectral chunks, approximately 400 chunks contain useful Doppler information, each giving an independent measure of the Doppler shift with an error of $\sim$200 m s^{-1}. Thus, the uncertainty in the mean velocity between 16 Cygni A and B is 10 m s^{-1}. We checked this measurement and its uncertainty by performing the entire exercise anew using superior spectra from 1997 November 15 and obtained a result of -530 m s^{-1}, which confirms both the value and uncertainty. We adopt the new radial velocity difference, $V_{B-A} = -530 \pm 10$ m s^{-1}.

We note that the small spectral type differences between the two spectra imply a slight mismatch in the fitting process. However, the resulting poor fits will produce randomly distributed errors in the Doppler shifts from each spectral chunk. The rms of the velocities of the $\sim$400 chunks is only 200 m s^{-1}, most of which is due to the finite S/N ratio of the spectra. Any spectral type mismatch would result in Doppler errors that are uncorrelated from one spectral chunk to the next, as new line blends will contaminate both the red and blue wings randomly. Therefore, the

TABLE 2

PHYSICAL PARAMETERS OF THE SUN AND 16 CYGNI A AND B

Parameter	Sun	16 Cygni A	16 Cygni B	Reference
Spectral Type	G2 V	G2 V	G5 V	1
$B-V$		0.643	0.661	1
T_{eff}	5770	5785 ± 25	5760 ± 20	1
		5750 ± 75	5750 ± 75	2
log g (cgs)	4.44	4.28 ± 0.07	4.35 ± 0.07	1
Mass ($M_\odot$)	1.0	1.046 ± 0.014	0.992 ± 0.012	3
[Fe/H]	0.0	$+0.05 \pm 0.06$	$+0.05 \pm 0.06$	1
		$+0.10 \pm 0.05$	$+0.09 \pm 0.05$	2
v sin i(km s^{-1})	1.9 ± 0.3	1.6 ± 1.0	2.7 ± 1.0	4
Rotation period (days)	25.38	26.9	29.1	5

REFERENCES.—(1) Friel et al. 1993; (2) Gonzalez 1997; (3) present work; (4) Soderblom 1982; (5) Hale 1994.

uncertainty in the mean velocity is constrained to better than 10 m s^{-1}. The gravitational redshift and the convective blueshift each vary from star to star, which could also affect our measured velocity of 16 Cygni B relative to A. Each effect amounts to a few hundred meters per second, and each varies with stellar mass no faster than linearly. Since the two stars differ by only a few percent in mass, these two effects imply the need for velocity corrections of a few meters per second. We do not make corrections for those effects here, as they would carry errors that are comparable in magnitude to the correction. Nonetheless, we presume that our relative velocity between A and B carries an additional uncertainty of ~ 10 m s^{-1}.

Finally, the proper motion of the binary system causes a secular increase in the radial velocity caused by changing geometrical perspective of the velocity vector. This acceleration is given by

$$dV_r/dt = 0.0229\mu^2/\pi_P \text{ m}^{-1} \text{ s}^{-1} \text{ yr}^{-1} ,$$

where μ is in arcsec yr^{-1} and π_P is the parallax in arcsec. For 16 Cygni this amounts to 0.044 m s^{-1} yr^{-1}, which is negligible here.

4. STELLAR MASSES

We now estimate the masses of the two stars, 16 Cygni A and B. There are various ways to estimate stellar masses from photometry and spectroscopy, and here we employ spectral type and $B-V$ as mass proxies. We adopt the mass scale devised by Gray (1992). The stars 16 Cygni A and B are classified as G2 V and G5 V, respectively, which yields masses of 1.06 and 0.98 $M_\odot$. The $B-V$ values, given in Table 2, along with Gray's (1992) color-mass calibration yield slightly different masses. Averaging these masses with those from the spectral type calibration yields final masses for the stars of $M_A = 1.046 \pm 0.014$ and $M_B = 0.992 \pm 0.012\ M_\odot$, as listed in Table 2.

Metallicity could alter the mass estimates. Metal-rich stars suffer greater line blanketing and have altered energy generation rates and opacities. Friel et al. (1993) and Gonzalez (1997) found that the ratio of iron to hydrogen is solar in both 16 Cygni A and B, within the uncertainties. Gonzalez also examined the total metallicity of 16 Cygni B and deduced a value of [M/H] = +0.09. This indicates that 16 Cygni may be slightly metal rich and hence that 16 Cygni A and B may be slightly more massive than listed in Table 2. Gonzalez (1997) estimated the 16 Cygni A and B masses to be 1.03 ± 0.04 and $1.01 \pm 0.04\ M_\odot$, respectively, which agree, within the uncertainties, with our estimates. The uncertainty in the stellar masses of several percent does not significantly alter the final orbital parameters derived here. The weakness of the lithium lines (King et al. 1997) and the weak chromospheres (Friel et al. 1993) in 16 Cygni AB indicate that the system is slightly older than the Sun, consistent with near solar metallicity.

5. TWO-BODY PROBLEM SOLUTION

We describe here a technique for determining a binary orbit when only the instantaneous position and velocity vectors are available, along with the stellar masses. The velocity components in the plane of the sky, V_x and V_y, come directly from the astrometry, and V_z comes from the difference in the radial velocity between 16 Cygni A and B. These velocities are essentially instantaneous, as the duration of the astrometric measurements spans only 150 yr, relative to the orbital period of $\sim$30,000 yr. Indeed, no significant curvature is detected in the astrometry, as seen in Figures 1 and 2.

One can almost determine the full position vector of B relative to A, with x and y (plane of the sky) coming from astrometry. This leaves undetermined only the line-of-sight component of the position vector between the two stars, z. This is the distance to 16 Cygni B perpendicular to the plane of the sky containing component A.

We constrain the value of z by the condition that the orbit be bound. As mentioned in § 4 and shown in Table 2, 16 Cygni A and B have similar spectral types and nearly the same metallicity. It is therefore highly plausible that these two stars coevolved from the same material and are a binary system. Based on the assumption that this is a binary system, the limiting potential energy relative to the measured kinetic energy is

$$E = \frac{1}{2}\mu v^2 - \frac{GM_A M_B}{r} < 0 , \quad (5)$$

where μ is the reduced mass, v is the velocity of B relative to A, and G is the gravitational constant.

The resulting acceptable values of z for a bound orbit are

$$-1375 < z < +1375 \text{ AU} . \quad (6)$$

We calculate the orbital parameters as a function of z, as constrained above, which is identical to employing the current separation, r, as the independent variable (Romanenko 1994). This approach yields a family of possible orbits. Future astrometric measurements will further constrain z, eventually restricting this family of orbits. We now describe the approach by which orbital solutions are achieved.

The constants of motion, energy, and angular momentum, are parameterized in the usual way:

$$E = -\frac{GM_A M_B}{2a} \quad (7)$$

$$L^2 = GM_A M_B a(1 - e^2) , \quad (8)$$

where E is the total energy and a is the relative semimajor axis of B about A. For a chosen value of z, the instantaneous energy, E, is established from equation (5), thus determining the semimajor axis, a, from equation (7). The angular momentum, L, is determined below from the measured velocity and position of B relative to A, thus setting the eccentricity, e, from equation (8). The orbital period P is related to a via Kepler's third law:

$$P = 2\pi\left(\frac{a^3}{GM}\right)^{1/2} , \quad (9)$$

where M is the total mass.

The central potential implies that $\boldsymbol{L} = \mu[\boldsymbol{r} \times (d\boldsymbol{r}/dt)]$ is a constant of the motion, with magnitude invariant to rotations about the origin. We now define the angles that relate the projected positions on the plane of the sky to that in the plane of the orbit. By convention, the plane of the sky is adopted as a useful reference plane. The plane of the orbit is tilted relative to this plane by the inclination i. The angular momentum vector in the sky reference frame is given by

$$\boldsymbol{L} = \mu L \begin{pmatrix} \sin i \sin \Omega \\ -\sin i \cos \Omega \\ \cos i \end{pmatrix} , \quad (10)$$

where Ω is the longitude of the ascending node (Taff 1985, p. 34).

The orbital plane cuts the plane of the sky along the line of nodes. At the "descending node" the secondary mass approaches the plane of the sky from behind (positive z) and moves toward the observer (V_z is negative). The ascending node marks the point at which the secondary mass passes back through the plane of the sky, away from the observer (V_z is positive). Astronomical conventions dictate that north ($+\hat{\boldsymbol{x}}$) is up and east ($+\hat{\boldsymbol{y}}$) is to the left, and $+\hat{\boldsymbol{z}}$ points away from the observer. Note that a left-handed coordinate system applies: $\hat{\boldsymbol{x}} \times \hat{\boldsymbol{y}} = -\hat{\boldsymbol{z}}$. The angle Ω is measured in the plane of the sky from north through east to the ascending node.

We can rewrite $\boldsymbol{L}$ in Cartesian coordinates, and thereby relate i and Ω to the observable quantities $\{x, y, z, V_x, V_y, V_z\}$ via equation (10):

$$\boldsymbol{L} = \mu L \begin{pmatrix} yV_z - zV_y \\ zV_x - xV_z \\ xV_y - yV_x \end{pmatrix} . \quad (11)$$

Equating equation (10) to equation (11), we have the following relation for i:

$$i = \arccos (xV_y - yV_x) , \quad (12)$$

and Ω is given by

$$\Omega = \left\{ \begin{array}{l} \arcsin\left(\dfrac{yV_z - zV_y}{\sin i}\right) \\ \arccos\left(\dfrac{xV_z - zV_x}{\sin i}\right). \end{array} \right\} \quad (13)$$

The third angle needed to relate the plane of the orbit to the positions projected onto the plane of the sky is ω the *argument of periapse*. This orbital parameter is related to ϕ and the true anomaly v via

$$\omega = v - \phi , \quad (14)$$

where ϕ is the angle from the line of nodes to star B along the orbit, and v is the angle from periastron to B along the orbit. These set the location of the periastron with respect to the ascending node.

The last remaining orbital parameter is T_P, the *time of periastron passage*. When the secondary companion passes through periastron, $v = 0$ and $\boldsymbol{r} \cdot (d\boldsymbol{r}/dt) = 0$. The value of T_P is calculated as follows (Taff 1985, p. 34):

$$n(t - T_P) = 2 \arctan\left[\left(\frac{1 - e}{1 + e}\right)^{1/2} \tan\left(\frac{v}{2}\right)\right] - \frac{e(1 - e^2)^{1/2} \sin v}{1 + e \cos v} , \quad (15)$$

where n is the *mean motion* in radians per year, $n = 2\pi/P$, and t is the time of observation.

Quadrant ambiguity arises when inverse trigonometric functions are employed. There are various ways to check each angle. For the case of Ω, the quadrant is fixed with L_x and L_y. For example, if $L_x > 0$ and $L_y > 0$, then Ω could be in quadrant II or IV. 16 Cygni B is presently projected onto the plane of the sky in quadrant II (southeast of the primary). Since $V_z < 0$, 16 Cygni B is crossing through the plane of the sky from behind. Therefore, the *descending node* is in quadrant II. Ω is defined as the angle measured from north toward east to the *ascending node*. Therefore, Ω is in quadrant IV for this case. Similar tests are performed to fix the quadrant of v, ϕ, and therefore ω. All seven of the orbital elements $[P, a, e, i, \omega, \Omega, T_P]$ can now be computed from measurements. In the next section we apply this approach to 16 Cygni AB.

6. THE COMPUTED ORBIT OF 16 CYGNI

We now determine the orbital elements of 16 Cygni B relative to A, based on their masses and their relative position and velocity vectors. We use the measured values $[x, y, V_x, V_y, V_z]$ and a range for $z = [-1375, 1375$ AU], that ensures a bound orbit (§ 5) to calculate the complete family

of possible orbital parameters. A summary of the measured astrometric and velocity quantities for 16 Cygni AB are given in Table 3.

From these observed quantities and the orbital solution in § 5, the orbit is computed for various assumed values of z. Table 4 gives the orbital parameters for seven representative values of z, [−1300, −900, −450, 0, +450, +900, +1300 AU]. A graphical depiction of the orbital parameters as a function of the full range in z is displayed in Figure 5. Figure 5*a* shows the orbital sensitivity to the uncertainty in the parallax.

The computed orbits for 16 Cygni AB show that for mid-range values of z, i.e., $-900 < z < +900$ AU, the orbital period is between 18,000 and 90,000 yr, and the semimajor axis is between 877 and 2500 AU. The eccentricities are between 0.53 and 0.93. Thus the orbit appears to be quite eccentric for all values of z. For extremely large values of z, larger periods and semimajor axes are possible, with the limiting case being a barely bound orbit of infinite semimajor axis.

Motivated by the report of a possible M dwarf companion to 16 Cygni A (Trilling et al. 1998), we consider a case in which the primary star, 16 Cygni A, has an enhanced mass of $M_A = 1.4\ M_\odot$. Table 5 lists the computed orbital parameters as a function of z, for this hypothetical case. This case shows how the orbit would change if component A had a companion, 16 Cygni "C" of mass 0.35 $M_\odot$, with both A and C in orbit around 16 Cygni B. This enhanced-mass case yields orbits for AB that have systematically smaller semimajor axes by roughly 30%. (Increasing M_A causes the potential energy to become more negative, thus diminishing a by fractional amounts that depend on the total potential energy, which in turn depends on the assumed z.) Similarly, the periods are reduced by factors of roughly 50%. This period reduction can be understood from Kepler's third law for which a is reduced and the total system mass is greater.

For nearly unbound cases (i.e., large z), this hypothetical increase in M_A alters the predicted orbit nonlinearly. The resulting orbital parameters as a function of z, for enhanced M_A, are shown graphically in Figure 5*b*. We exhibit three trial mass enhancements of 0.50 $M_\odot$, 0.35 $M_\odot$, and 0.20 $M_\odot$ (added to its original mass of $M_A = 0.05\ M_\odot$). Each mass enhancement results in a different allowed range in z, owing to the requirement that the binary, AB, be bound. These new ranges in z are $z = [-1850, 1850$ AU], $z = [-1700, 1700$ AU], and $z = [-1575, 1575$ AU] corresponding to the three mass enhancements listed above. Apparently, the available astrometric and velocity data for 16 Cygni A and B are compatible with a bound and eccentric orbit for 16 Cygni A even if it harbors an unseen, low-mass companion of several tenths of a solar mass.

Since the astrometric and velocity measurements carry accompanying uncertainties, each orbital parameter [P, a, e, i, ω, Ω, T_P, r_{min}] is calculated for varying values of each measurement, as well as over the range in z. This gives the sensitivity of the orbital parameters to errors in the measured input values. Figure 5 shows not only how the derived orbital parameters vary over the range in z but also how they are affected by the uncertainty in the parallax, $\pi_P = 46.475 \pm 0.50$ mas. The parallax is the next most dominant term in the error budget, after the unknown value of z. In Table 6 we give the maximum departure of each orbital parameter from its nominal value, owing to measurement uncertainty.

We checked the derived orbital parameters for 16 Cygni AB by generating synthetic observable quantities. We used a Newton-Rhapson iteration technique to generate the orbital motion from the orbital parameters. The derived

TABLE 3

OBSERVABLES

Observable	Value	Uncertainty
ρ (arcsec)	39.338	0.0053
θ (deg)	133.44	0.014
$d\rho/dt$ (arcsec yr^{-1})	0.0126	0.00016
$d\theta/dt$ (deg yr^{-1})	−0.00768	0.00028
V_z (m s^{-1})	−530.0	15.0
M_A ($M_\odot$)	1.046	0.014
M_B ($M_\odot$)	0.992	0.012
M_C ($M_\odot$) ?	0.4	0.15
π_P (arcsec)	0.046475	0.00050

TABLE 4

COMPUTED ORBITAL PARAMETERS FOR 16 CYGNI B ORBITING A WITH ASSUMED z = 1300, 900, 450, 0, −450, −900, −1300 AU

Parameter	1300 AU	900 AU	450 AU	0 AU	−450 AU	−900 AU	−1300 AU
P (yr)	1310411.1	89099.5	27633.8	18212.2	27633.8	89099.5	1310411.1
a (AU)	15182.2	2529.2	1158.8	877.62	1158.8	2529.2	15182.2
e	0.901	0.585	0.609	0.862	0.930	0.892	0.960
i (deg)	101.56	105.23	113.38	135.44	148.98	118.05	107.98
ω (deg)	100.36	77.272	36.037	31.721	140.21	173.79	194.76
Ω (deg)	−64.869	−63.384	−59.850	−46.560	71.285	98.932	103.55
T_P (yr)	231.48	−1178.8	−1092.2	43.64	−85.31	−1273.3	−2615.6
Periastron distance (AU)	1503.2	1049.4	452.61	121.43	80.943	274.36	614.69

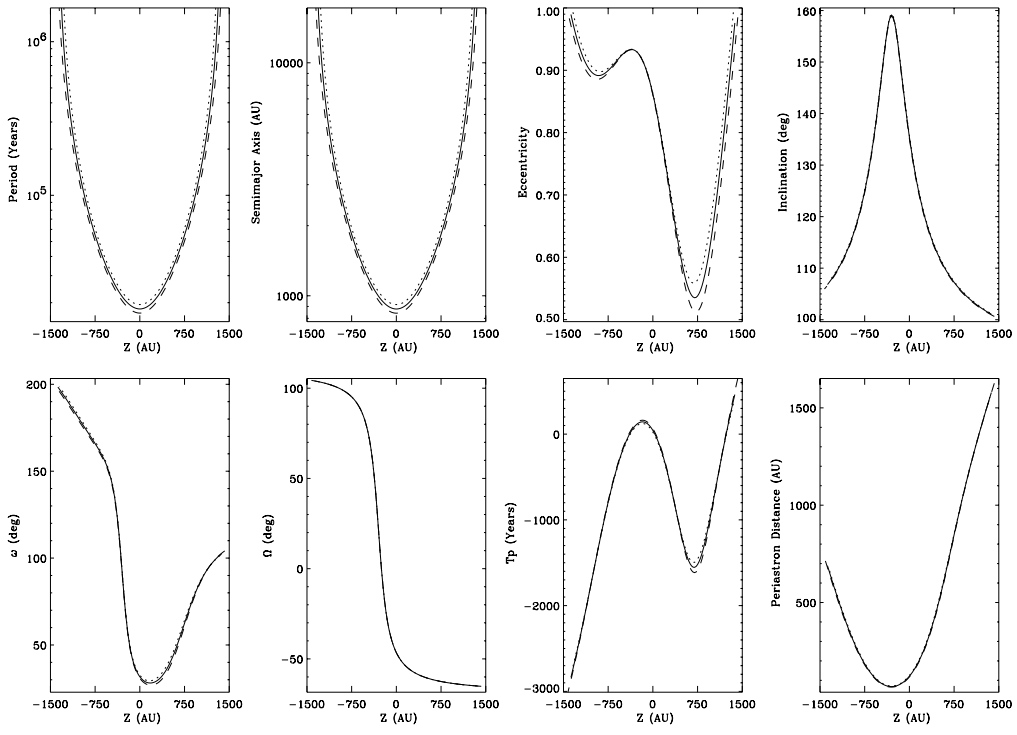

FIG. 5*a*

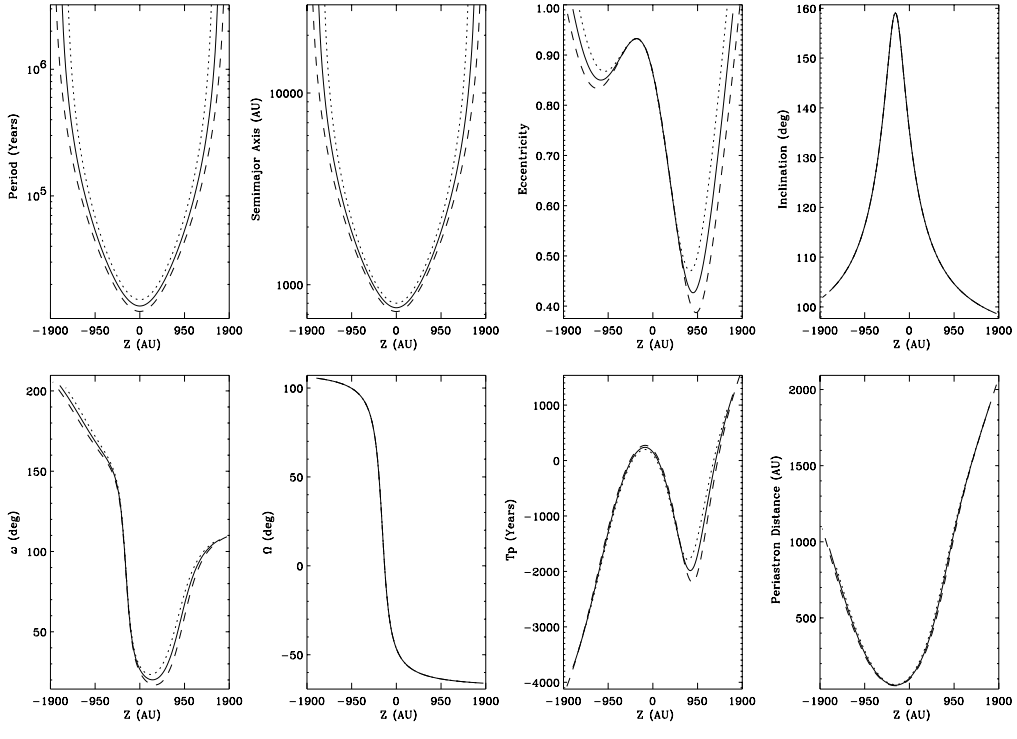

FIG. 5*b*

FIG. 5.—Orbital parameters as a function of the assumed line-of-sight separation, z, of 16 Cygni A and B. (*a*) Three plausible values of parallax are shown: $\pi_P = 45.975$ mas (*dotted line*), $\pi_P = 46.475$ mas (*solid line*), $\pi_P = 46.975$ mas (*dashed line*). (*b*) Orbital parameters of 16 Cygni B around a hypothetical combined mass, 16 Cygni (A + C). Three plausible values of the mass of the putative companion are shown: $M_C = 0.20\ M_\odot$ (*dotted line*), $M_C = 0.35\ M_\odot$ (*solid line*), $M_C = 0.50\ M_\odot$ (*dashed line*).

TABLE 5

COMPUTED ORBITAL PARAMETERS FOR 16 CYGNI B ORBITING THE COMPOSITE A+C WITH ASSUMED z = 1700, 1300, 900, 0, −900, −1300, −1700 AU

Parameter	1700 AU	1300 AU	900 AU	0 AU	−900 AU	−1300 AU	−1700 AU
P (yr)	23721972.	168568.4	46971.7	13512.7	46971.7	168568.4	23721972.
a (AU)	110350.4	4078.7	1740.1	758.29	1740.1	4078.7	110350.4
e	0.988	0.634	0.429	0.863	0.863	0.865	0.991
i (deg)	99.301	101.56	105.23	135.44	118.05	107.98	103.11
ω (deg)	107.38	95.648	61.294	26.600	166.38	185.27	203.37
Ω (deg)	−65.762	−64.869	−63.384	−46.560	98.932	103.55	105.56
T_P (yr)	1190.9	−144.37	−1849.9	153.25	−1120.9	−2544.6	−3730.2
Periastron distance (AU)	1891.0	1492.4	993.30	103.53	237.68	551.23	956.50

synthetic astrometric and velocity values agreed with the observed quantities, within measurement errors, i.e., the reduced χ^2 was unity.

One benefit of this check is that we can synthesize the full orbit in the plane of the sky as well as in the plane of the orbit. Figures 6*a* and 6*b* show 16 Cygni B's orbit about A projected onto the plane of the sky for five values of z. Figure 6*c* shows the orbit for the hypothetical case in which component A has an enhanced mass of $1.05 + 0.35 = 1.4$ $M_\odot$, displayed for the same three z values as in Figure 6*b*. Apparently, if component A has the enhanced mass, the shape and orientation of the orbits are similar to the nominal case, shown in Figure 6*b*, but the orbital size is reduced by typically ∼30%.

Without a refinement of z, the orbit of 16 Cygni is likely to remain uncertain, despite future improvements in astrometric quantities. The small clump of data points in Figure 6 illustrates how short the astrometric data string is relative to the size of the orbit. See Figure 7 for an expanded view showing the agreement between the derived orbits and the astrometric data.

7. A LOW-MASS COMPANION TO 16 CYGNI A?

Coronographic images of 16 Cygni A have recently revealed a stellar source located $3''.2 \pm 0''.2$ away, and follow-up adaptive optics images confirm the existence of this star (Trilling et al. 1998). Its physical association with 16 Cygni A remains unknown. Here, we will refer to this prospective new companion of 16 Cygni A as component "C." If C resides at the same distance as A, the projected separation, AC, is 70 AU, and the mass of C would be, $M_C = 0.4 \pm 0.15\ M_\odot$ (Trilling et al. 1998).

TABLE 6

UNCERTAINTY IN AN ORBITAL PARAMETER, IF z WERE KNOWN

Orbital Parameter	Uncertainty	Primary Cause
P (yr)	3821	Parallax
a (AU)	97.5 AU	Parallax
e	0.009	Parallax
i (deg)	0.549	$d\theta/dt$
ω(deg)	1.19	$d\rho/dt$
Ω (deg)	0.616	$d\theta/dt$
T_P (yr)	19.3	Parallax
r_{min} (AU)	6.62	V_z

The predicted orbit of the wide binary 16 Cygni AB would be significantly modified by C owing to several effects. The combined mass of AC, ∼1.4 $M_\odot$, would orbit component B. In § 6 and Table 5 we describe the new orbit of 16 Cygni AC about B due to the "enhanced" mass of A. The AB orbit would be smaller by roughly 30%. Figure 5*b* shows the resulting orbital parameters for AB, assuming that A has a total mass, $M \sim 1.4\ M_\odot$. Figure 6*c* shows the resulting projected orbit of B relative to A, for three values of z: −900, 0, and +900 AU. This figure should be compared to Figure 6*b*, which shows the projected orbit for nominal stellar masses of 1 $M_\odot$, for the same three possible values of z. Clearly the enhanced mass of A and C yields smaller orbits for B.

Another effect caused by the putative 16 Cygni C is its gravitational perturbations of A. The measured astrometric motion of component B relative to A could be caused in part by motion of A about C. The perturbations imposed on A by C can be estimated. If component C is gravitationally bound to A, then one would expect a reflex velocity and acceleration of A. We estimate this perturbation by adopting an true distance between AC of $(3/2)^{1/2}$ greater than the projected separation, yielding $r \approx 85$ AU. This estimated distance is similar to the estimated semimajor axis, 100 AU, that stems from the prescription of Couteau (1960).

7.1. Radial Velocities of Component A due to C

We first adopt a trial circular orbit for C about A with orbital radius of 85 AU. The orbital velocity of A about the center of mass of AC is

$$V_{orb} = 1100 \frac{M_C}{0.4\ M_\odot} \sqrt{\frac{1.45\ M_\odot}{M_A + M_C}}\ \text{m s}^{-1},$$

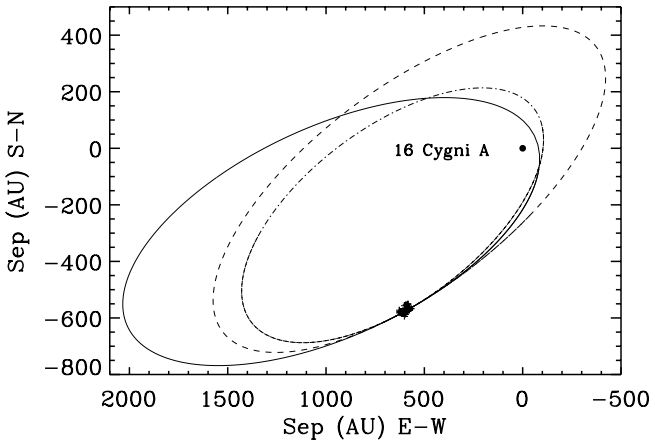

FIG. 6*a*

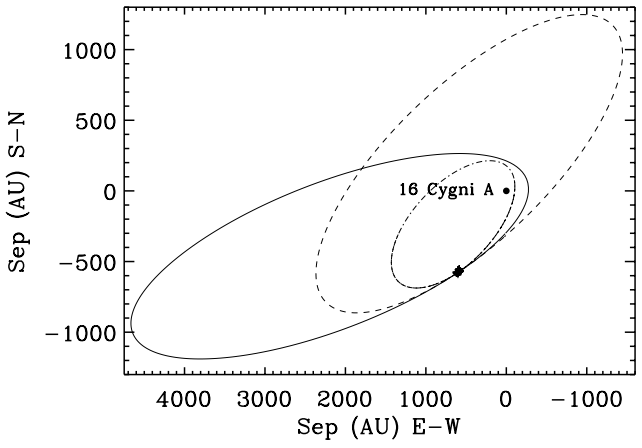

FIG. 6*b*

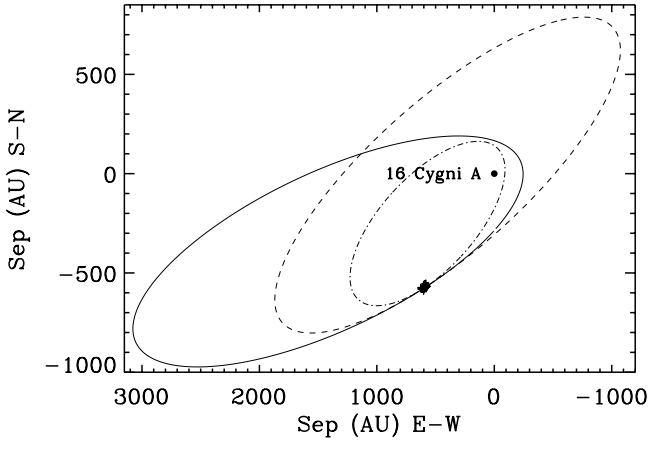

FIG. 6*c*

FIG. 6.—Orbit of 16 Cygni B relative to A, projected onto the plane of the sky, for assumed line-of-sight separations, z, of 16 Cygni A and B. (*a*) $z = 450$ AU (*dashed*), $z = -450$ AU (*solid*), $z = 0$ AU (*dash-dotted*). (*b*) $z = 900$ AU (*dashed*), $z = -900$ AU (*solid*), $z = 0$ AU (*dash-dotted*). (*c*) Orbit of B about the hypothetical composite mass of A + C (1.4 $M_\odot$) for $z = 900$ AU (*dashed*), $z = -900$ AU (*solid*), $z = 0$ AU (*dash-dotted*). The astrometric data are plotted as the clump of crosses located where the three orbits overlap. North is up, and east is to the left.

and the orbital period of AC is $P = 700$ yr (for assumed masses of 1.05 and 0.4 $M_\odot$).

This period is so long that the full velocity amplitude of 1100 m s^{-1} would not have been realized during the 11 yr of velocity measurements. Nonetheless, the radial velocity of A might have changed during the past 11 yr owing to its orbit about C. The lack of an orbital phase prevents a precise prediction of dV_r/dt. Instead, we compute the rms value of dV_r/dt of A due to C:

$$dV/dt_{\rm rms} = 7.0 \times \sin i \ {\rm m\ s^{-1}\ yr^{-1}}\ .$$

This expected velocity slope varies with the assumed masses as $M_C/(M_A + M_C)^{3/2}$ and with the distance between A and C as $1/r^2$. Here, i is the unknown orbital inclination of the AC orbit. Thus, we anticipate that 16 Cygni A should exhibit a change in radial velocity of $\sim 7 \sin i$ m s^{-1} yr^{-1}, if this new component C is truly bound to A.

We have examined our velocities of 16 Cygni A (see Fig. 3) for evidence of this velocity trend. The early two velocities in 1987 carried systematic errors of ~ 30 m s^{-1}. Since then, the velocities of 16 Cygni A exhibit a downward trend with a slope of -5.1 ± 1.5 m s^{-1} yr^{-1} (weighted linear fit). This trend appears to be real at a level of 3 σ and thus should be considered suggestive.

Systematic errors in velocity measurements over the course of 11 yr could explain this trend. Therefore, we estimated the systematic errors by using the residuals to the Keplerian fit to 16 Cygni B (Fig. 4). Plausibly, those residuals would reflect systematic errors that were common to both stars, caused by instrumental effects. The corrected velocities for 16 Cygni A are also shown in Figure 3 and have a downward trend of -4.1 ± 1.5 m s^{-1} yr^{-1} (weighted fit), significant at a level of 2.7 σ. We are concerned that the neighboring star 3.″2 away from 16 Cygni A

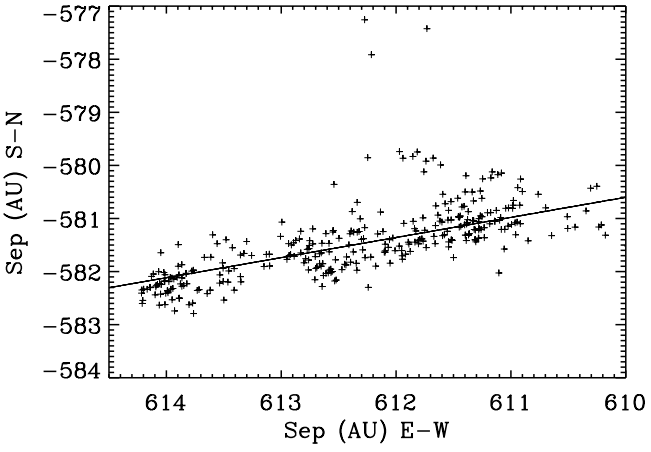

FIG. 7.—Expanded view of Fig. 6, showing the agreement between the computed orbit (*diagonal line*) for 16 Cygni AB and the astrometric data from 1962 to 1982. All assumed line-of-sight separations, z, for 16 Cygni A and B yield computed orbits that are coincident with the diagonal line.

may have contaminated the spectra of it, thus introducing additional velocity errors that depend on image rotation, seeing, and guiding. Thus, the downward velocity trend in 16 Cygni A may be spurious.

This observed slope of -4.1 m s^{-1} yr^{-1} in the velocities of 16 Cygni A is consistent with the rough expectation from above for the effects of component C on A. The apparent slope cannot be due to secular acceleration, $+0.05$ m s^{-1} yr^{-1}, caused by the geometrical trading of proper motion for radial velocity. The observed velocity trend also greatly exceeds the change in the velocity of 16 Cygni A due to its orbit about 16 Cygni B, which would be no more than 0.2 m s^{-1} yr^{-1} (see Fig. 9). Thus, the slope in the velocities of 16 Cygni A is consistent with the suggestion that component C is indeed bound to A.

7.2. Astrometric Accelerations of Component A due to C

We now test the hypothesis that component C is bound to A by searching for the expected acceleration of A during the past 160 yr. Note immediately that in Figure 2, the separation of A and B, ρ versus t, exhibits no significant curvature to the eye. This suggests that A suffered no observed acceleration during 160 yr.

We now place quantitative limits on any acceleration of A by using the relative positions of A and B dating from 1830 (Figs. 1 and 2). The astrometric accuracy was $\pm 0\farcs2$ in the 1800s and was $0\farcs02$ from 1950 to the present. This astrometry provides positions and transverse velocities for A relative to B. In addition, *Hipparcos* provides astrometric positions and proper motions for A relative to B. The linear extrapolation of all ground-based measurements to the epoch 1991.25 accurately predicts the relative positions of A and B that were measured by *Hipparcos* to within 3 mas. Thus, all astrometric measurements are self-consistent.

The acceleration of A due to the force exerted by C has two astrometrically observable components, declination (decl) and right ascension. Trilling et al. (1998) report that A is nearly due north of C, which implies that the acceleration on A should be greatest in the southward direction. From Newtonian physics, the acceleration of A in the north-south direction is

$$a_{\rm decl} = -0.0024(89\ {\rm AU}/r)^2(M_{\rm C}/0.5\ M_\odot)\ {\rm AU\ yr}^{-2}\ .$$

Here, we have scaled the result for r, the distance from A to C, and for $M_{\rm C}$, the mass of C.

Thus, the force on A caused by C implies an expected dec acceleration of 0.0024 AU yr^{-2}.

We have measured the actual dec component of the acceleration of A relative to B. Note that the binary AB should produce no detectable curvature or acceleration in their relative separation during 150 yr (see orbital fit in Fig. 7). However, the AB separation should reflect the acceleration of A due to C, assuming C is really bound to A. We have measured this acceleration of A in the declincation direction by measuring the first derivative, dx/dt at different epochs. (We use x for declination.)

The instantaneous relative velocity in declination of A and B measured by *Hipparcos* at 1991.25 is

$$dx/dt = 0.100 \pm 0.003\ {\rm AU\ yr}^{-1}\ .$$

We also measured dx/dt from the ground-based astrometry at two epochs:

At 1966,

$$dx/dt = 0.095 \pm 0.015\ {\rm AU\ yr}^{-1}\ .$$

At 1880, from the astrometry from the period 1830–1930,

$$dx/dt = 0.115 \pm 0.025\ {\rm AU\ yr}^{-1}\ .$$

Apparently, the decl component of the relative velocity of AB has not changed significantly from 1880 to the present.

Taking differences in the above velocities between 1880 and 1991.25 (*Hipparcos*), one finds the observed acceleration is 0.00014 ± 0.00022 AU yr^{-2}, consistent with no acceleration. The upper limit to the dec acceleration, 0.00036 AU yr^{-2}, is 6.7 times smaller than that predicted from Newton's Laws, 0.0024 AU yr^{-2}. This conflict yields a clear constraint on star C.

As a check, 22% of the nominal 720 yr orbit should have transpired since 1830. But the astrometry shows no hint of any curvature in the motion of A. Indeed, if the orbit were circular, A would have traced a quarter-circle arc having a length of $\sim 1''$, which is clearly not the case, as seen in the linear astrometry in Figure 2.

One possible resolution is that the putative 16 Cygni C resides 2–3 times farther behind or in front of A than the projected separation, i.e., it resides ~200 AU from A. Such a separation would be only 4 times smaller than the projected separation of A and B (830 AU), thus rendering component C vulnerable to dynamical disruption from B. An alternative resolution is that the mass of C is less than $\sim 0.25\ M_{\odot}$, thereby diminishing the expected acceleration of A. Some combination of both solutions is possible. In either of these cases, we are forced to conclude that the radial velocity slope of -4.1 ± 0.5 m s^{-1} yr^{-1} is spurious. If C is so distant or low-mass to avoid astrometric acceleration, then it cannot explain the marginal radial velocity slope, either. The lack of astrometric acceleration leaves open the possibility that C is a background star.

8. DISCUSSION

The lack of detectable astrometric acceleration of A during 160 yr suggests that only two stars, 16 Cygni A and B, dominate the dynamics of the system. The marginal acceleration of component A along the line of sight, $dV_r/dt = -4.1 \pm 1.5$ m s^{-1} yr^{-1}, could be caused by contamination of the spectrum of A by the nearby star (Trilling et al. 1998), whether it is bound to A or not. Indeed, the velocity trend of component A could reflect its proper motion relative to the nearby star. Thus, 16 Cygni is likely to be well described dynamically as a simple binary.

Our nominal, predicted orbit of 16 Cygni AB has orbital parameters with the following ranges: $P > 18{,}200$ yr, $a > = 877$ AU, $e = 0.54$–1, and $i = 100°$–160°. The periastron distance is 68–1579 AU, and the recent time of periastron passage is $T_p = -2764$ to $+387$ yr. The above orbital parameters correspond to all possible bound orbits for which $1375 < z < 1375$ AU, at the extreme values of which the semimajor axis is infinite, which is clearly unphysical. We do not know the probability distribution for z. But binary orbits with $a > 0.075$ pc are extremely rare, as they are vulnerable to disruption by passing stars and molecular clouds (Poveda et al. 1994; Mallada & Fernandez 1996). Thus we consider more probable the restricted range $-1300 < z < 1300$ AU, which yields semimajor axes smaller than 0.075 pc. These orbits have $18{,}200 < P < 1.3$ Myr, $877 < a < 15{,}180$ AU, and periastron distances $68 < r_p < 1500$ AU. The above values represent the most likely orbital parameters for 16 Cygni AB.

Our computed orbital parameters are similar to those found by Romanenko (1994) and Kiselev & Romanenko (1996). They found likely values for orbital elements of $a = 1219$–3266 AU, $P = 30{,}000$–132,000 yr, and $e = 0.78$–0.96. Our values and quadrants of i, ω, and Ω also agree with Romanenko's results if 90° is added to their inclination values. Note that we also found that the periastron passage occurred within a few thousand years of the present. The differences in our results are attributable to the new astrometric and velocity data.

Kiselev & Romanenko (1996) adopted a radial velocity difference of -940 ± 260 m s^{-1}. This artificially high speed for 16 Cygni B relative to A forced a reduced range of allowed z values to ensure a bound orbit. The inflated speed propagates through to the orbital parameters. In particular, the higher kinetic energy, for a given value of z (and hence given potential energy), results in a larger period and semimajor axis. The approximate agreement between their orbital parameters and ours is understandable, however, because the dominant source of uncertainty stems from the unknown line-of-sight distance between stellar components A and B. We have constrained this line-of-sight distance by demanding that the binary orbit be gravitationally bound. The kinetic energy is known well now, from the improved radial velocity, thus restricting the instantaneous potential energy of the system and hence constraining z. Thus, our family of orbits for 16 Cygni represents the latest refinement in its determination.

Holman et al. (1997) and Mazeh et al. (1997) examined the possibility that 16 Cygni A exerts sufficient gravitational influence on the planetary companion, 16 Cygni Bb, to account for its eccentricity ($e = 0.69$). Holman et al. (1997) discuss the effects at two possible periastron ($r_{\rm min}$) distances of 100 and 500 AU. The eccentricity of the planet's orbit oscillates between near zero and ~0.75 on a timescale of 100 Myr for the shortest possible periastron distances.

We find that the stellar binary periastron distance lies between 68 and 1500 AU for almost the entire allowed range of the line-of-sight separation of AB, namely for $-1300 < z < +1300$ AU. This range of periastron distances implies a large range of possible oscillation periods, $P_{\rm osc}$, for the planet's eccentricity. We compute the oscillation period from the relation in Holman et al. (1997):

$$P_{\rm osc} = P_{\rm PL}\left(\frac{M_{\rm A}}{M_{\rm B}}\right)\left(\frac{a_{\rm BIN}}{a_{\rm PL}}\right)^3 (1 - e_{\rm BIN}^2)^{3/2}\ , \qquad (16)$$

where $P_{\rm PL} = 2.2$ yr is the period of the planet, $M_{\rm A} = 1.046\ M_{\odot}$ is the mass of the primary star, $M_{\rm B} = 0.992\ M_{\odot}$ is the mass of the secondary star, $a_{\rm BIN}$ is the semimajor axis of the stellar binary system, $a_{\rm PL} = 1.7$ AU is the semimajor axis of the planet, and $e_{\rm BIN}$ is the eccentricity of the binary orbit.

The resulting periods of eccentricity oscillation for the planet range from 22 Myr for $z = +250$ AU up to 440 Gyr for $z = -1350$ AU. Figure 8 shows the oscillation period as a function of the relative line-of-sight distance between 16 Cygni B and A. The age of the 16 Cygni binary system is likely to be 5–10 Gyr, based on its weak lithium (King et al. 1997), slow stellar rotation (Hale 1994), and position on the H-R diagram (Gonzalez 1998). Soderblom et al. find an age

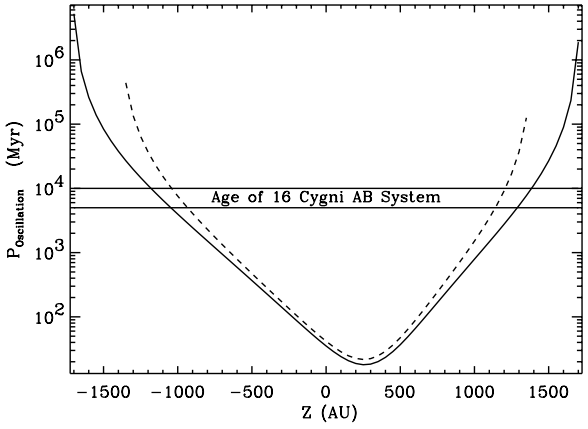

FIG. 8.—Theoretical periods of eccentricity oscillation for the planet, 16 Cygni Bb, as a function of the assumed line-of-sight separation, z (and implicitly the periastron distance), of 16 Cygni B from A with its nominal mass (*dashed line*) and with a hypothetical augmented mass of 1.4 $M_\odot$ (*solid line*). The horizontal lines bracket the plausible age range, 5–10 Gyr, for 16 Cygni. Values of z between -1000 AU and $+1200$ AU yield oscillation periods less than the lifetime of the stellar system. Outside that range of z, the eccentricity of the planet around 16 Cygni B cannot be explained by perturbations from 16 Cygni A.

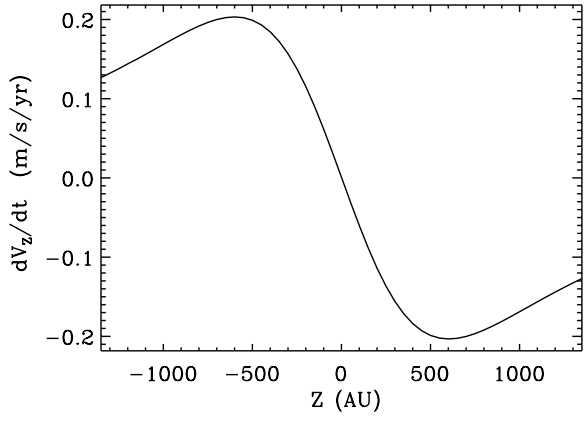

FIG. 9.—Instantaneous time derivative of the radial velocity of 16 Cygni B with respect to A as a function of the assumed line-of-sight separation, z.

of 8.9 Gyr, and the chromospheric emission at Ca II H&K indicates an age of 7 Gyr.

The oscillation period is less than the age of the binary system for 77% of the range in z, thus enabling significant evolution of the planet's eccentricity. The perturbation mechanism should be assessed carefully for greater periastron distances of 500–1900 AU. However, it appears that only the timescale, and not the amplitude, of the eccentricity variations of the planet is sensitive to the periastron distance (Holman et al. 1997).

The lack of curvature in the astrometric data prevents us from constraining further the range of allowed values of z beyond [-1375, 1375 AU]. The radial velocity for each star is predicted to vary by only, $dv/dt < 0.1$ m s^{-1} yr^{-1} (Fig. 9), which remains below measuring threshold. Future astrometry at a precision of ~ 1 μas, should reveal the curvature in the orbit, thereby constraining the orbital parameters. Additional Doppler data may also reduce the range of z if a definitive trend is detected (assuming no component C is bound). Figure 9 shows that if a positive velocity trend is detected, the positive values of z are ruled out, while a negative trend implies that the negative z values are not allowed.

The possible M dwarf companion to 16 Cygni A reported by Trilling et al. (1998) defies a clear interpretation at this time. The available astrometry suggests that A has not suffered any perturbation from this star, which indicates one of three possibilities: (1) The companion is at least 200 AU from A, (2) it has mass less than 0.25 $M_\odot$, or (3) it is a background star. The correct interpretation of C may come from improved spectroscopy and photometry or from an assessment of its comoving status with the 16 Cygni system.

However, if this companion does reside 100–200 AU from 16 Cygni A, then a large fraction of the family of orbits for 16 Cygni AB would be vulnerable to exclusion, notably those that carry component B within ~ 1000 AU of A. Indeed, most of the members of the family of orbits of 16 Cygni AB have periastron distances less than 1000 AU. It is just these potentially excluded orbits that can drive the eccentricity of the planet around B. Thus, the putative component C would significantly diminish the parameter space within which the eccentricity of the planet could be driven by component A. If C is bound to A, the oscillation time for the planet's eccentricity might exceed the lifetime of the 16 Cygni system. Clearly, if C is bound to A, careful three-body calculations will be required to ascertain the plausible orbits of 16 Cygni A and B.

9. CONCLUSION

We have explored all of the possible orbits for 16 Cygni, given the available astrometric and velocity data, and a modern *Hipparcos* parallax. The orbital parameters were calculated from a short astrometric arc ($<1\%$) of the full orbit and from a modern value of the difference in the radial velocity between the two stars. The dominant uncertainty comes from the unknown distance, z, of star B in front of, or behind, the plane of the sky that passes through A. This range in z is constrained by the condition that the orbit be gravitationally bound, which leads to a family of possible orbits.

The orbit of star B about A has a period $P > 18{,}200$ yr, a semimajor axis $a > 877$ AU, and an eccentricity $e = 0.54$–1. The semimajor axis is unlikely to exceed 0.1 pc to ensure stability in the Galactic environment, which thus further constrains the plausible orbital parameters. The resulting likely periastron distances are $68 < r_p < 1500$ AU. The orbital parameters found here represent significant

improvements over those found by Romanenko (1994) and Kiselev & Romanenko (1996), and differences are due to the improved astrometry, velocities, and parallax.

Given the revision in orbital parameters, some reassessment of the perturbations of the planet, 16 Cygni Bb, would be valuable, especially for binary orbits of large semimajor axis. We wonder if extreme periastron distances of 1290 AU actually induce significant amplitudes in eccentricity with supposed periods of $\sim$3.5 Gyr as suggested by Mazeh et al. (1997) and Holman et al. (1997). One wonders what other perturbers could gravitationally supersede this mechanism, such as other planets or Kuiper belts.

We also use the velocities of 16 Cygni A and the relative astrometry of A and B to assess the membership and plausible orbits of the putative M dwarf companion, component "C," to 16 Cygni A (Trilling et al. 1998). The velocities show a marginally credible trend that is consistent with this companion being bound. But the astrometry does not exhibit the acceleration of component A expected from the gravitational perturbations of component C. This suggests that component C is considerably farther from A than the projected distance or that it has a mass below $\sim 0.25\ M_{\odot}$. In such cases, the orbit of 16 Cygni AB computed here would be approximately correct, despite the third body. Nonetheless, if C is bound to A, it serves as a sensor of the periastron distance of 16 Cygni AB, excluding close passages within $\sim$1000 AU. Such a constraint restricts further the parameter space within which the eccentricity of 16 Cygni Bb could be driven by component A.

The suggestion that the extraordinary eccentricity of the planet stems from the perturbations of star A remains viable. To determine if the planetary orbit and stellar binary have the requisite relative inclination, further work on the rotational inclination of 16 Cygni B (via $V \sin i$) should be carried out as a proxy for the orbital inclination of the planet (see, e.g., Hale 1994). Meanwhile, further extrasolar planet candidates have now been discovered that have equally large orbital eccentricities. The stars HD 210277 and HD 168443 have apparent planetary companions with orbital eccentricities greater than 0.5, and both appear to be single stars (Marcy et al. 1998). The M dwarf, Gliese 876, has a planetary-mass companion ($M \sin i = 2.0\ M_{\rm JUP}$) with an eccentricity of 0.27. Thus orbital eccentricities among Jupiter-mass companions may arise without stellar companions.

We thank Paul Butler for his integral role in initiating the project and for all Doppler measurements. We are grateful to C. Worley for astrometric data. We thank Debra Fischer, Mario Savio, Eric Williams, Chris McCarthy, and Phil Shirts for observations at the Lick Observatory telescopes. We thank A. Irwin for a careful reading of the manuscript. We also thank M. Holman, S. Tremaine, and W. D. Cochran for valuable discussions. We thank D. Trilling and M. Liu (1998, private communication) for advance news about the star near 16 Cygni A. This work was done in partial fulfillment of the requirements for the master's degree for H. Hauser at San Francisco State University. Funding was provided by NSF (AST 9520443), NASA (NAGW 5125), and Sun Microsystems. We thank the University of California and Lick Observatory for generous allocation of resources for these observations.

REFERENCES

Artymowicz P. 1998, in ASP Conf. Ser. 134, Brown Dwarfs and Extrasolar Planets, ed. R. Rebolo, E. L. Martín, & M. R. Zapatero Osorio (San Francisco: ASP), 152
Bevington, P. R., & Robinson, D. K. 1992, Data Reduction and Error Analysis for the Physical Sciences (2d ed.; New York: McGraw-Hill)
Butler, R. P., Marcy, G. W., Williams, E., McCarthy, C., Dosanjh, P., & Vogt, S. S. 1996, PASP, 108, 500
Cochran, W. D., Hatzes, A. P., Butler, R. P., & Marcy, G. W. 1997, ApJ, 483, 457
Couteau, P. 1960, J. des Observateurs, 43, No. 3
Friel, E., de Strobel, C., Chmielewski, M. S., Lebre, A., & Bentolila, C. 1993, A&A, 274, 825
Gonzalez, G. 1997, MNRAS, 285, 403
———. 1998, A&A, 334, 221
Gray, D. F. 1992, The Observation and Analysis of Stellar Photospheres (2d ed., Cambridge: Cambridge Univ. Press)
Hale, A. 1994, AJ, 107, 306
Holman, M., Touma, J., & Tremaine, S. 1997, Nature, 386, 254
Irwin, A. W., Yang, S. L. S., & Walker, G. A. H. 1996, PASP, 108, 580
King, J. R., Deliyannis, C. P., Hiltgen, D. D., Stephens, A., Cunha, K., & Boesgaard, A. M. 1997, AJ, 113, 1871
Kiselev, A. A., & Romanenko, L. G. 1996, Astron. Rep., 40, 795
Mallada, E., & Fernandez, J. A. 1996, Rev. Mexicana Astron. Astrofis., Ser. de Conf., 4, 103
Marcy, G. W., & Butler, R. P. 1998, AR&A, in press
Marcy, G. W., Butler, R. P., Vogt, S. S., Fischer, D. A., & Liu, M. 1998, ApJ, submitted
Mazeh, T., Krymolowsky, Y., & Rosenfeld, G. 1997, ApJ, 477, L103
Perryman, M. A. C., et al. 1997, A&A, 323, L49
Poveda, A., Herrera, M. A., Allen, C., Cordero, G., & Lavalley, C. 1994, Rev. Mexicana Astron. Astrofis., 28, 43
Romanenko, L. G. 1994, Astron. Rep., 38, 779
Soderblom, D. 1982, ApJ, 263, 239
Taff, L. G. 1985, Celestial Mechanics (New York: John Wiley & Sons)
Trilling, D., Brown, R. H., & Liu, M. 1998, preprint.
Van den Bos, W. H. 1962, Stars and Stellar Systems, 2, Astronomical Techniques ed. W. A. Hiltner (Chicago: Univ. of Chicago Press), Chap. 22
Vogt, S. S. 1987, PASP, 99, 1214